Spiralling around

Marie-Pascale Corcuff
e-mail: m-p.c@wanadoo.fr

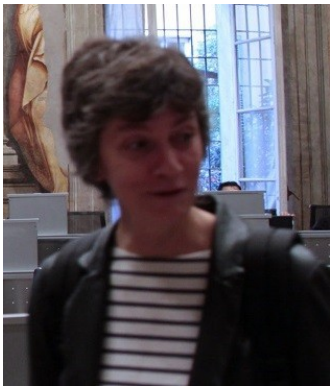

Abstract

Spirals are everywhere in nature. Phyllotactic spirals have particularly attracted the attention of scientists such as biologists and mathematicians, but also artists, including architects.

Much has been discussed about phyllotactic spirals, in particular the emergence of parastichy pairs of spirals in consecutive Fibonacci numbers. Here, after showing a dynamical model capable of displaying all features of phyllotactic spirals, we will take a step aside, by describing, analysing, and generalising non-phyllotactic spirals appearing in ancient Roman mosaics tessellating disks. This will lead us to a transformation from square to disk, which translates Cartesian coordinates into polar ones, in at least two ways, and to the consideration that spirals are as much generic to this centred geometry as straight lines are to our more familiar one.

Then, spiralling back to phyllotaxy, we will show the transition between the concentric spiral patterns, and proper phyllotactic patterns. We will wonder what type of genetic spiral may be chosen, and what it changes about the resulting conspicuous spirals.

1. Phyllotactic spirals: a basic dynamic model

I already tackled the topics of phyllotactic spirals in my paper for GA2018 [1], by digitally simulating the analogue experiment made by Douady and Couder [2]. I used this experiment as an example of some distant force, here magnetic repulsion, creating interesting forms, here phyllotactic spirals. Douady and Couder invented an apparatus consisting in drops of ferrofluid falling at the centre of a dish filled with silicone oil and placed in a vertical magnetic field which repels the drops from the centre. The centre of the dish has a small bump, so that *a priori* the drops fall in a random direction, and continue in that direction until they reach the edge of the dish (where they fall into a ditch). But the drops are repelled from each other as well, so that the direction of each new drop depends on the repelling effect of one or more of the previous ones. A first emergent phenomenon takes place: a steady regime of divergence (the angle between the direction of two successive drops) appears, which leads to the fact that the drops are points of a spiral, the generative or genetic spiral.

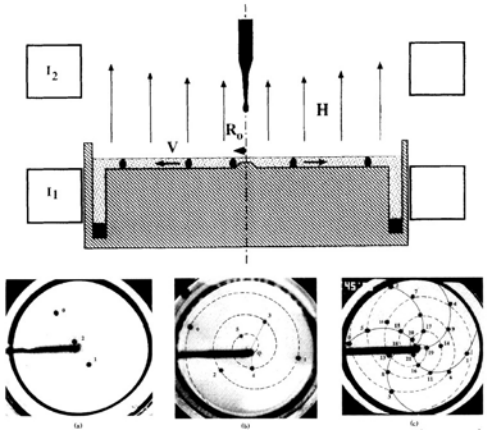

Fig. 1: Douady and Couder experiment

For some divergence angles, a second emergence occurs, which is the one we admire in sunflowers and many other phyllotactic spirals: what we perceive is not the genetic spiral itself, but secondary spirals, which happen to be in consecutive Fibonacci numbers.

Two parameters are involved in this experiment: the periodicity of the falling of drops, and the initial velocity of the drops. The constant divergence angle emerges whatever the choice of parameters, however phyllotactic spirals emerge only for some values of the parameters.

In my algorithmic model, particles are created at the centre at regular times, and travel in a straight line towards the periphery. The direction of the two first particles is random, but after that, the direction of each particle is determined by the position of all the previous particles, according to the law of magnetic repulsion. The absolute value of the speed of each particle is set at a given value, and does not change in time, nor its direction, once it is determined. The particles travel from the centre to the periphery along a radius, with the same constant speed. Douady and Couder acted upon the periodicity of the fall of drops, because it was the easiest to adjust, but I chose to align the creation of particles with the frame rate in processing, so the parameter upon which I act is the absolute value of the speed.

The first few particles act in a chaotic way but, rapidly, a constant divergence angle between consecutive particles emerges, giving way to spirals. For some value of the speed, the famous $360 / \varphi^2 \approx 137.5\ °$ (where $\varphi = (1+\sqrt{5})/2$ is the golden mean) divergence angle appears, and produces the phyllotactic spirals we are familiar with. A slight change in the given speed

will produce so-called degenerate spirals.

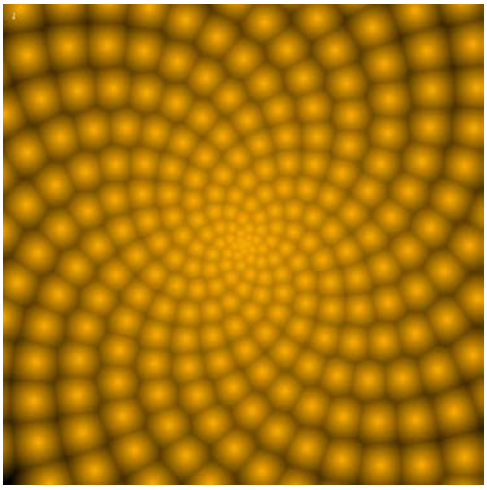

Fig. 2: Overall pattern

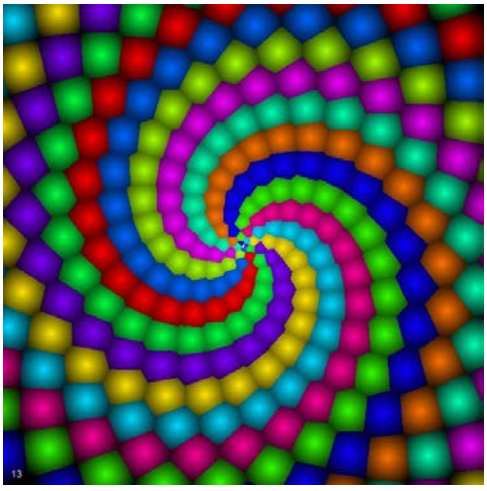

Fig. 3: 13 clockwise spirals

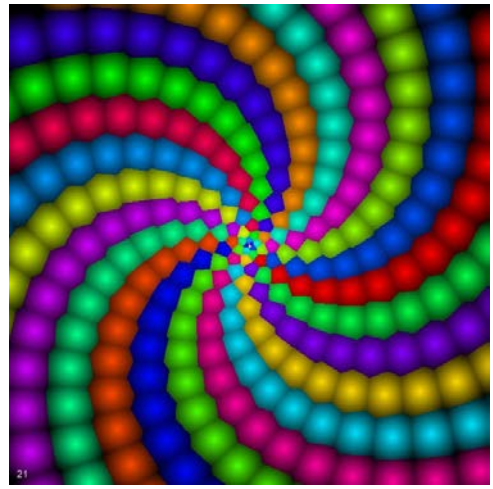

Fig. 4: 21 anti-clockwise spirals

As efficient as this model seems to be – it is dynamic, it provides phyllotactic spirals without explicitly using the "noble" divergence angle, which is what we expect if we do not subscribe to any teleology or intelligent design – it is not without providing some more questions: what would be the equivalent system of repulsion in a botanical organism (as obviously it would not be magnetism), and moreover, does not deciding on a given absolute value of speed instead of the divergence angle simply displace the teleological problem? As not a botanist, I shall not try to answer those questions, which have been amply discussed among more competent scientists.

However, this model has got all the constituents of the phenomenon of emerging phyllotactic spirals observed in botanical nature: there is a **genetic** or **generative spiral** formed by consecutive particles separated by a constant **divergence angle** and, more importantly, with the right speed, this model displays **visible** or **conspicuous parastichy pairs** of spirals in **consecutive Fibonacci numbers**.

2. Non phyllotactic spirals in concentric tessellations

2.1 Ancient Roman mosaics: description and analysis

All spirals are not phyllotactic, which means that spirals may be seen without any genetic spiral. So I was very surprised to find this illustration in the “bible” of phyllotaxis [3]:

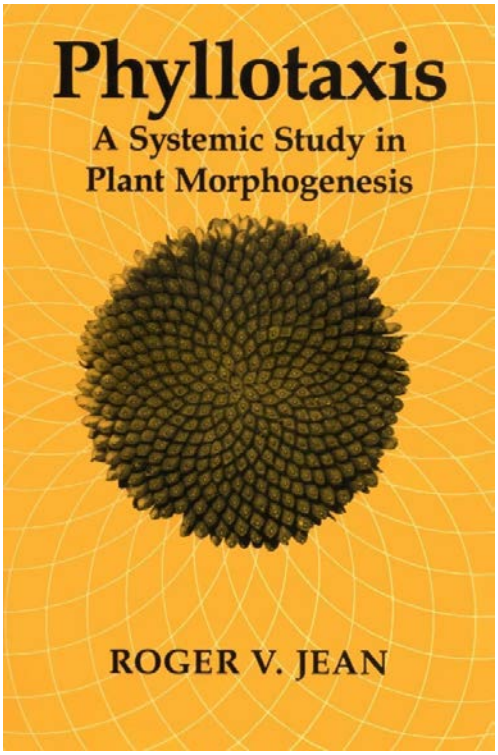

Fig. 4

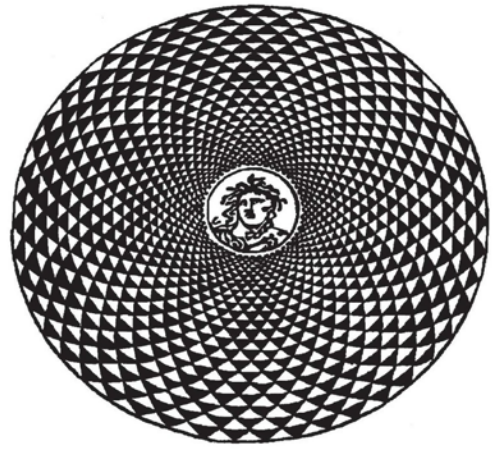

Fig. 5: [3] p. 234

It is actually a bad reproduction of the ancient Roman mosaic shown in Fig. 6:

Fig. 6: Roman mosaic with Head of Medusa, 115–150 AD. Museo Nazionale Romano—Palazzo Massimo alle Terme.

This mosaic looks very much like this other one, but with the head reversed:

Fig. 7: Mosaic Floor with Head of Medusa, 115-150 AD. J. Paul Getty Museum

The principle of this mosaic is simple: triangles are put regularly along concentric circles around a centred ornated disk, and layers are offset from each other, in a quincunx pattern.

Other mosaics obey the same logic, like those:

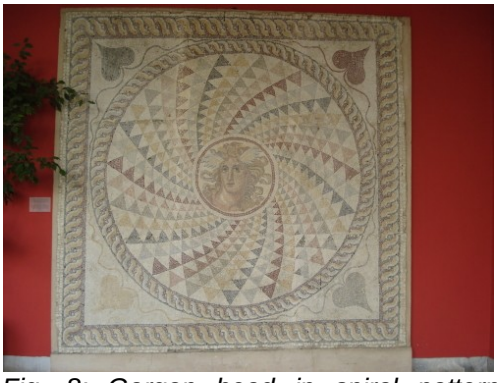

Fig. 8: Gorgon head in spiral pattern mosaic. Archaeological Museum, Athens.

Fig. 9: Spiral pattern mosaic. Palazzo Massimo Museum, Rome.

where emerging spirals are enhanced, or this one:

Fig. 11: Head of Dionysos in spiral pattern mosaic. Corinth, Greece.

where spirals in both directions are enhanced.

All mosaics above show triangles with size increasing with the radius, which makes them roughly isometric. But there is at least one exception to this rule:

Fig. 12: Roman geometric mosaic roundel, circa 3rd Century AD.

which does not prevent the emergence of spirals…

Other mosaics show spirals emerging from concentric quadrilateral shapes, without the quincunx:

Fig. 13: Roman mosaic, Syria, circa 4th-5th century AD.

Fig. 14: Roman mosaic, Antioch, circa 400 AD.

Those spirals are certainly not “phyllotactic”, and Fibonacci numbers have nothing to do with them. There is no genetic spiral, there are as many spirals as there are shapes around the central disk, all concentric layers have the same number of shapes, and lastly, there are as many spirals in one direction as in the other one.

We can analyse the patterns made of triangles according to the number of triangles in each layer, and to the number of layers (which happens to be the number of triangles in each conspicuous spiral).

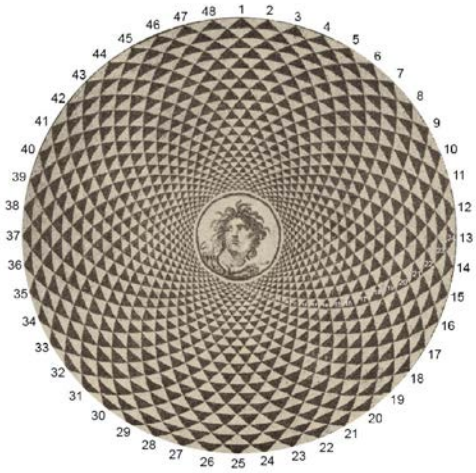

Fig. 15: 48 triangles by layer, 24 layers

Fig. 17: 38 triangles by layer, 10 layers

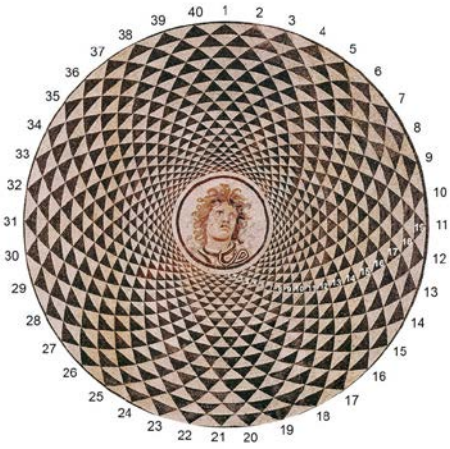

Fig. 16: 40 triangles by layer, 19 layers

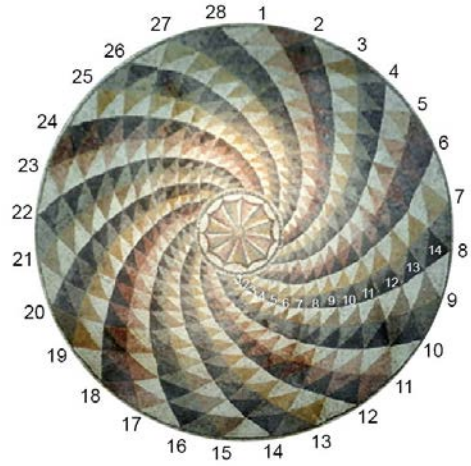

Fig. 18: 28 triangles by layer, 14 layers

This analysis ascertains that those two mosaics are very different, even if they look alike at first glance.

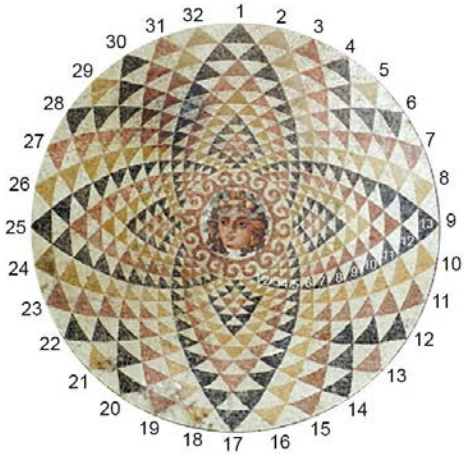

Fig. 19: 32 triangles by layer, 13 layers

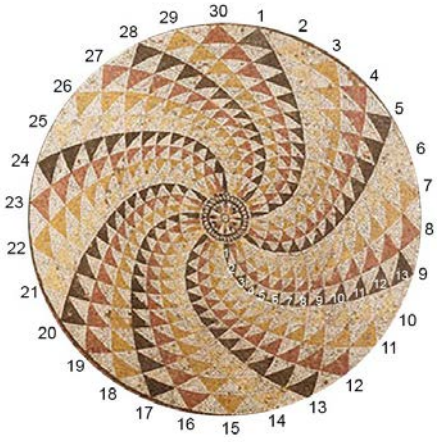

Fig. 20: 30 triangles by layer, 13 layers

The first mosaic with squarish shapes is much less elaborate, the mosaicist has struggled with the pattern in some parts, the difficulty being that one must make roughly squarish shapes of different sizes, each size corresponding to a constant fraction of the changing perimeter, and all that with a very small number of fixed size pieces... It is a relevant example of the conflict between discrete (the pieces of stone) and continuous (the fraction of the perimeter), or between integer and real numbers...

The pattern starts in a rather straightforward way. The mosaicist has managed to place 63 2-by-2 squares around the inner disk. But things go bad at a certain point and there are only 61 squarish shapes at the boundary...

Fig. 21: 61- 63 squares by layer, 7 layers

Faced with the same problems, the rabbit mosaicist managed rather well…

Fig. 22: 48 squares by layer, 4 layers

Let us now try and make our own idealized version of those patterns. One must take into account the way in which the height of the triangle or quadrilateral shape, i. e. the width of the annular layer, varies from centre to boundary. Without direct access to the original mosaics, it is difficult to exactly measure it. But in most cases, if not the result, at least the intent of the artist seems to be that all triangles are isometric. In one case (Fig. 12, 20), the height is approximately constant. As the base of the triangle is defined by the perimeter of the central disk and the number of triangles, once the initial type of triangle and the number of layers are chosen, the whole pattern is determined.

Applying this method for our two first first mosaics, this is what it provides:

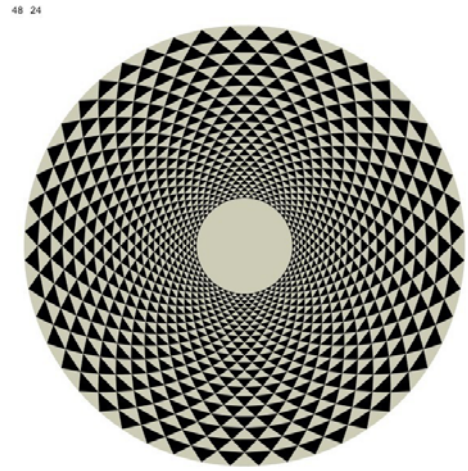

Fig. 23: cf. Fig. 6, 15.

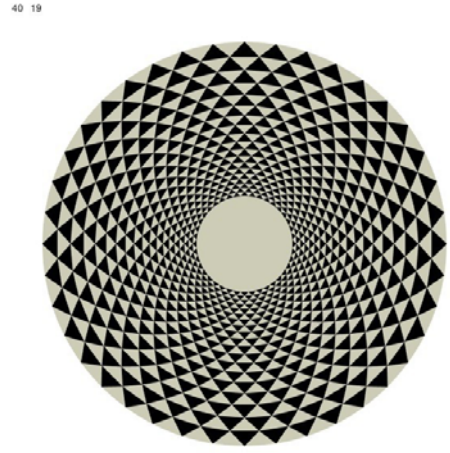

Fig. 24: cf. Fig. 7, 16.

The most compliant to the isometric model is the Gorgon (Fig. 8, 17), and it is also our first example of enhancing the spirals by colour. The mosaicist has encountered a problem with this attempt: by choosing 38 shapes surrounding the disk, he could not properly arrange the colours periodically (as 38 = 2x19, and 19 is a prime number). Anyway, here is our rendition of this pattern:

Fig. 25: cf. Fig. 8, 17.

The next mosaic shows spirals whirling in the opposite direction:

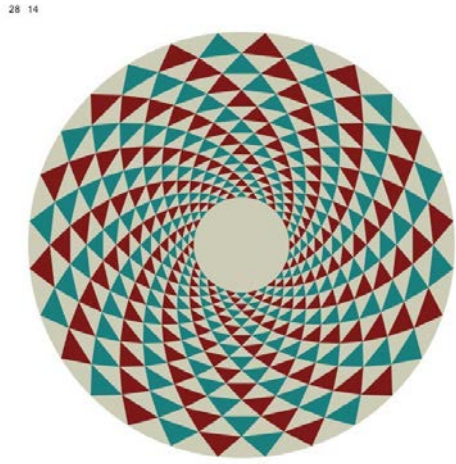

Fig. 26: cf. Fig. 9, 18.

The colouring of the next mosaic is more tricky, but by adjusting the numbering of the triangles, we manage to obtain this:

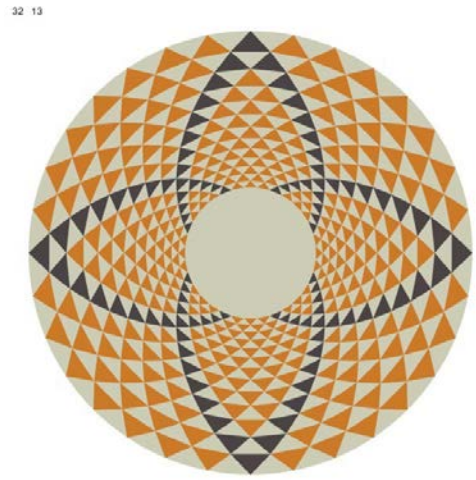

Fig. 27: cf. Fig. 11, 19.

Remains the 6th mosaic, where the triangles of the first layer around the central disk are very elongated, while the last ones at the boundary are more squat. It is not clear what the progression actually is based upon, but we shall assume that the intent was that all layers would be of the same width, all the triangles of the same height, regardless of their base.

Once again, the mosaicist has encountered a problem with the colouring of the spirals, or maybe he wanted some irregularity. Having chosen 30 shapes by layer, it would have been logical to make 5 sequences of 6 colours, or 6 sequences of 5 colours, but there are 6 sequences of 4 colours, and 2 of 3 colours. We shall be more rational, and opt for 6 series of 5 colours…

Fig. 28: cf. Fig. 12, 20.

The mosaics with quadrilaterals do not have the quincunx arrangement. Spirals are not so conspicuous, unless one colours consecutive shapes differently. Here are approximations of the two mosaics:

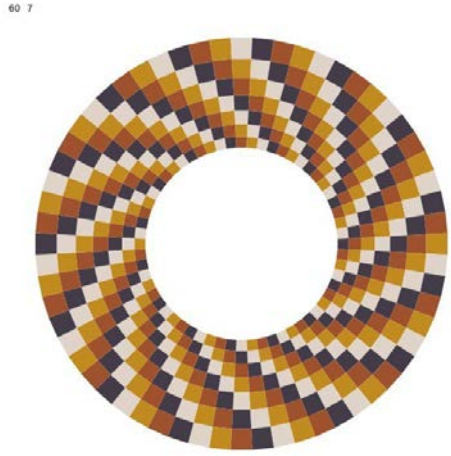

Fig. 29: cf. Fig. 13, 21.

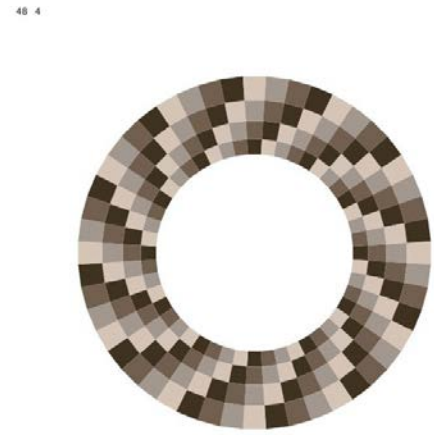

Fig. 30: cf. Fig. 14, 22.

2.2 Generalisation

All those mosaics do not tile an entire disk, but rather a ring, they all have a disk at the centre, decorated with a mythologic figure.

But, ideally, one can tile a disk in a similar way, by packing concentric layers of a given number of regularly distributed shapes. We simply divide the perimeter of any circle by the number of shapes we desire. The width of each layer depends upon the rule we choose to implement, the most natural being that the shapes are isometric. Obviously, there is a problem at the centre, where the perimeter tends to 0, as does the width of each shape… So we cheat a little, by starting with a radius of 1 instead of 0.

For instance, the tiling disk equivalent to the first mosaic we analysed is this:

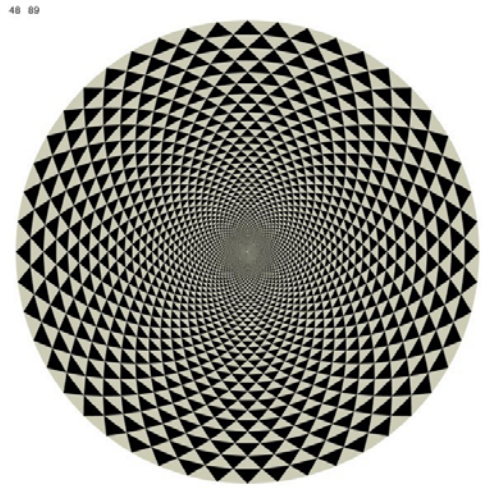

Fig. 31: Generalisation of Fig. 24.

but we note that it needs much more layers: 89, instead of 24.

We can now generalise this construction by choosing any number of shapes we want (for triangles we consider only the black ones), and letting the layers go as far as we want, and enhancing one of the generated spirals. The depth of each layer may be such that shapes are isometric, or it can be constant:

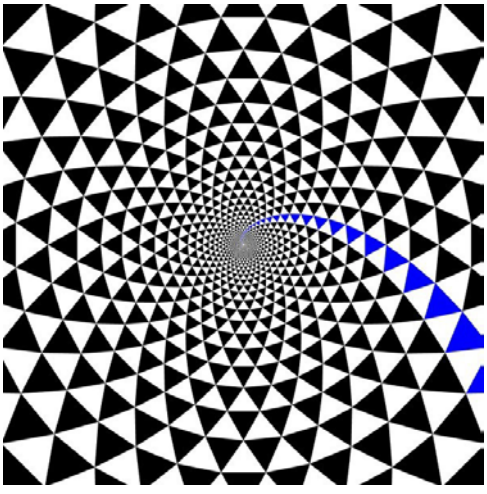

Fig. 32: 32 shapes, varying depth.

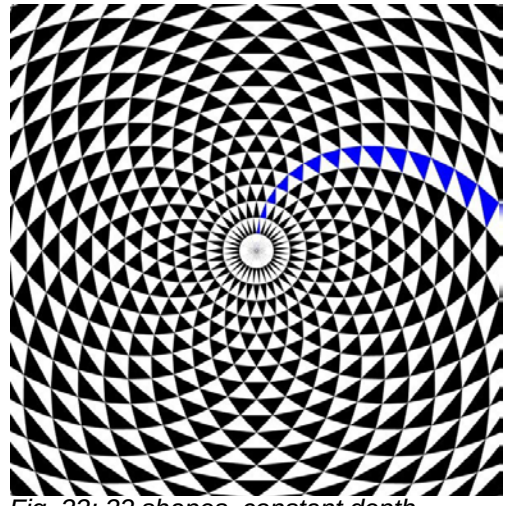

Fig. 33: 32 shapes, constant depth.

The same generalisation can be made with the quadrangles (all quadrangles are counted, both white and black):

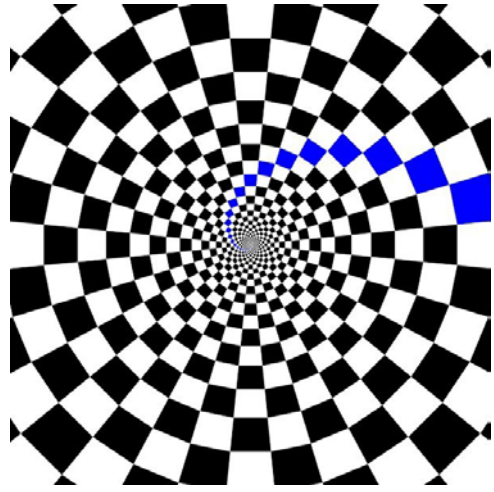

Fig. 34: 32 shapes, varying depth.

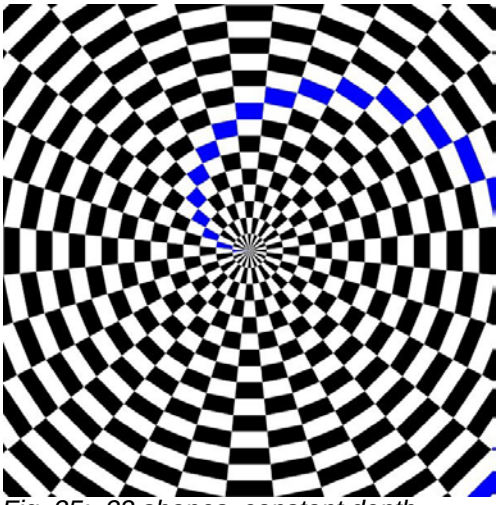

Fig. 35: 32 shapes, constant depth.

We can extrapolate our method to the other archetypal tiling of the plane, beside the triangular and orthogonal ones, the hexagonal. We need three colours in this case, and even without enhancing any spiral, they are rather conspicuous:

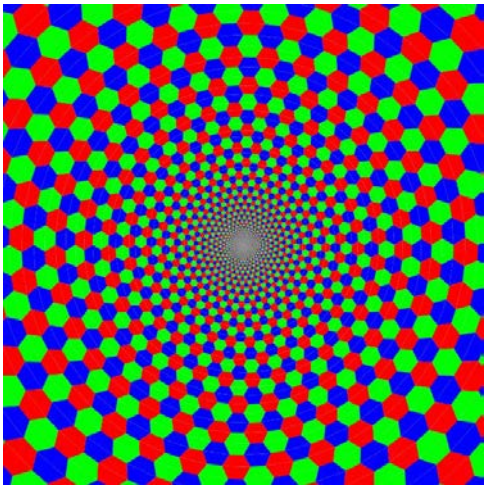

Fig. 36: 32 shapes, varying depth.

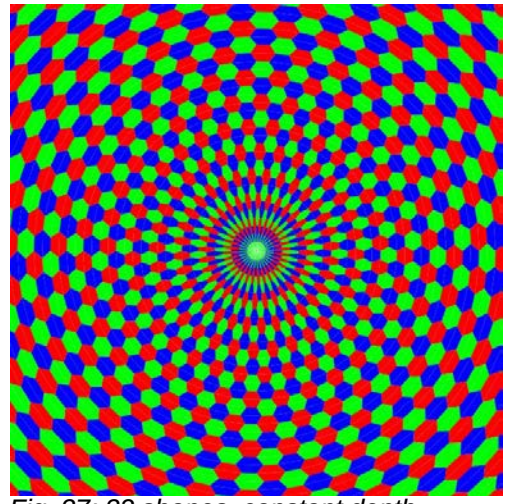

Fig. 37: 32 shapes, constant depth.

We must now return to our analysis of the mosaics with triangles and correct it. We had only considered the upward triangles, and observed that they were “in quincunx”. This assumption was in accordance with the mosaics, because the downward triangles, between the coloured ones, were left in a neutral colour, like a background. But for a more accurate analysis we must also consider the downward triangles. With a small number of (black) triangles we can see more clearly what actually happens, i. e. that the triangles lay on a hexagonal lattice:

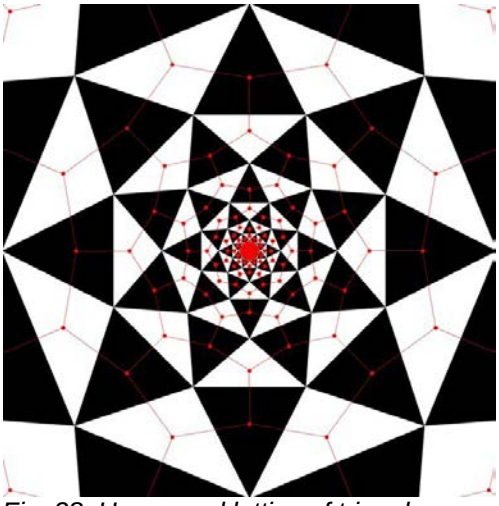

Fig. 38: Hexagonal lattice of triangles

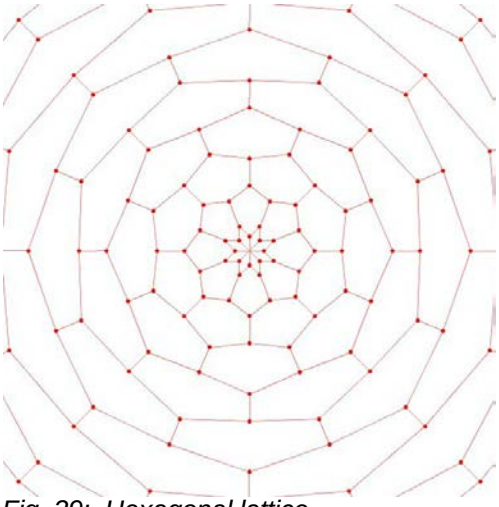

Fig. 39: Hexagonal lattice

Fig. 40: Hexagonal lattice of triangles

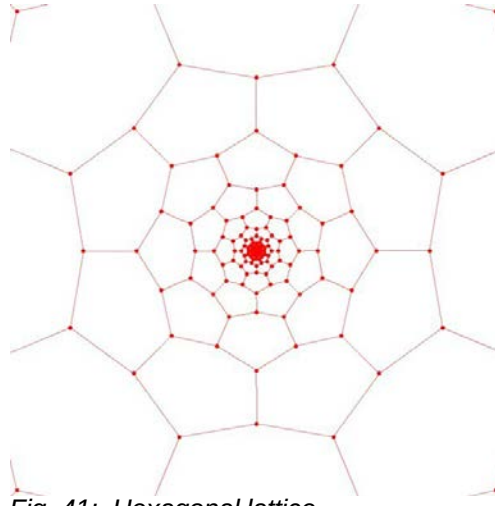

Fig. 41: Hexagonal lattice

We can now generate all particle patterns corresponding to possible tessellations, depending upon the type of lattice (“orthogonal”, triangular, hexagonal) and the variation (dr) of the radius of the particle positions.

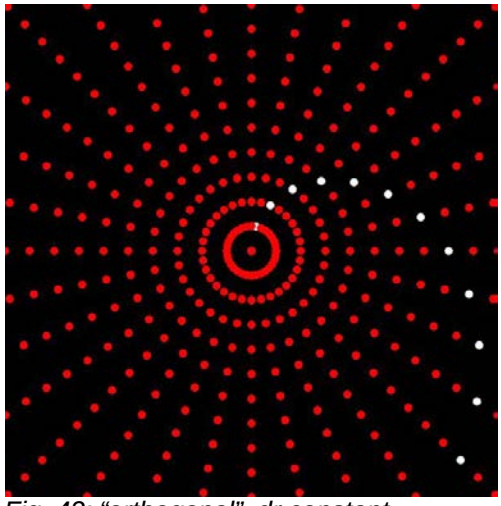

Fig. 42: “orthogonal”, dr constant.

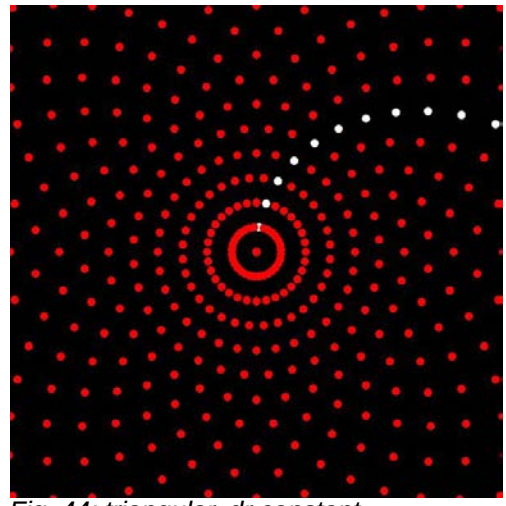

Fig. 44: triangular, dr constant.

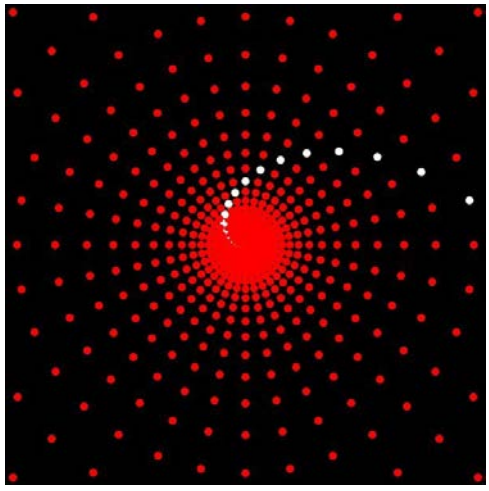

Fig. 43: “orthogonal”, dr variable.

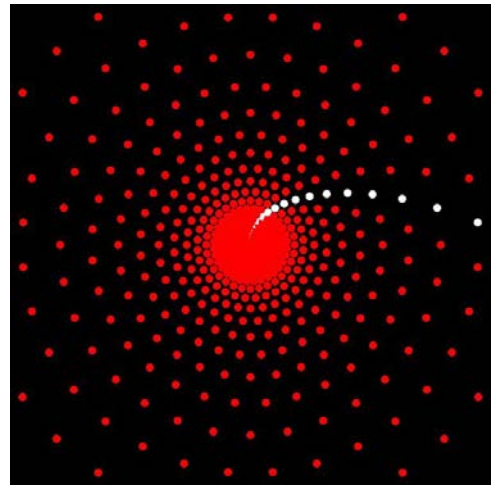

Fig. 45: triangular, dr variable

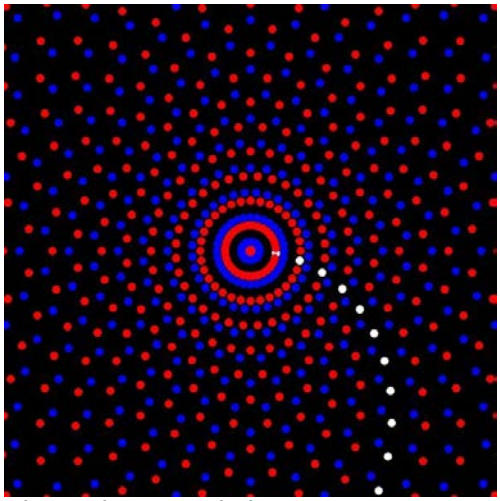

Fig. 46: hexagonal, dr constant.

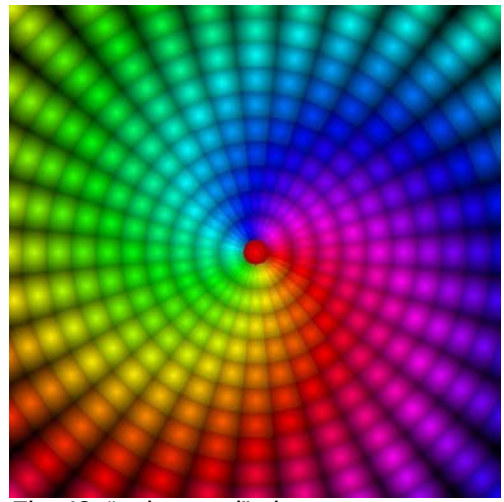

Fig. 48: “orthogonal”, dr constant

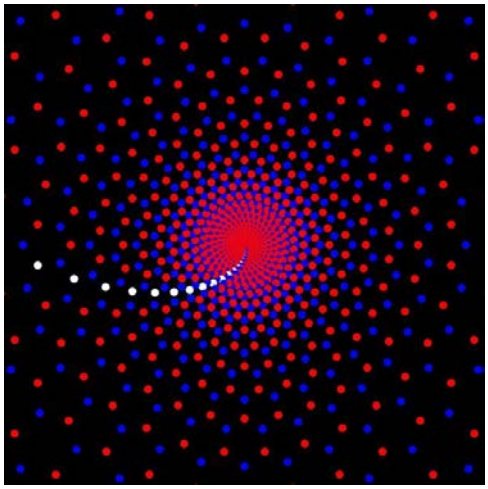

Fig. 47: hexagonal, dr variable

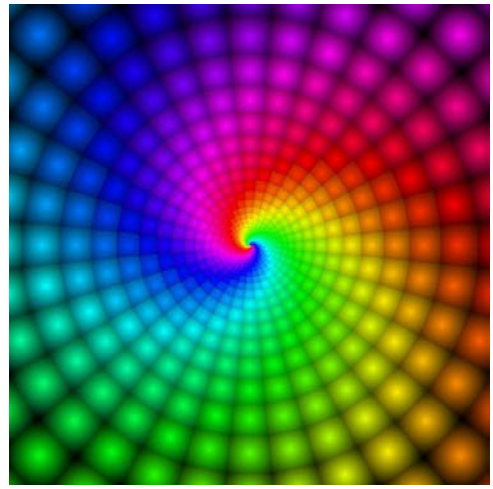

Fig. 49: “orthogonal”, dr variable

Now let us use these particles as sites for Voronoi tessellations:

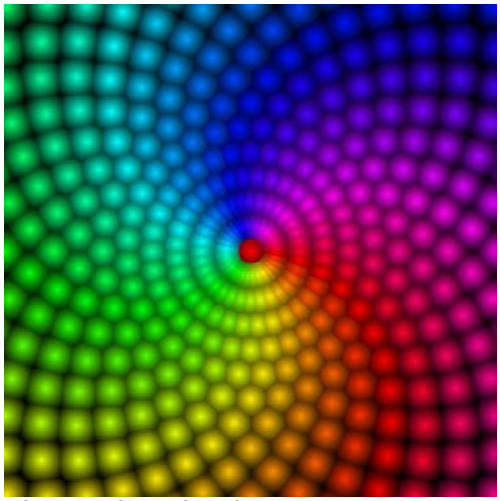

Fig. 50: triangular, dr constant

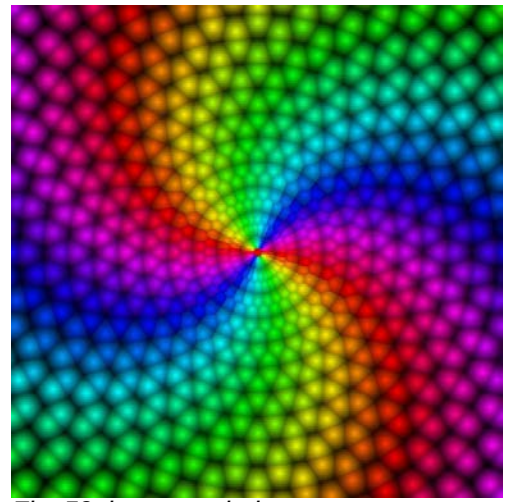

Fig. 52: hexagonal, dr constant

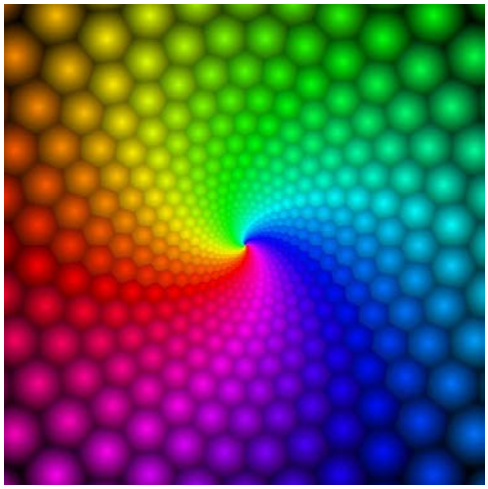

Fig. 51: triangular, dr variable

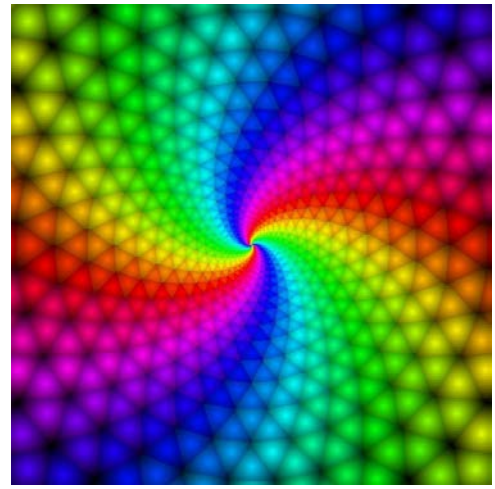

Fig. 52: hexagonal, dr variable

We notice that, in the case of the triangular and hexagonal lattices, while when dr is variable the tiles of the Voronoi tessellation are what we expect (hexagons and triangles, respectively) it is not always the case when dr is constant.

We could explore further this question, but it would lead us too far from our purpose, so in order to better explore the correspondence between our familiar tessellations and this new world of concentric tessellations, we shall make a little detour.

2.3 Cartesian to polar transformation

Tiling a disk is a task equivalent to tiling a rectangle, with a change of perspective, or, more accurately, of geometry.

We can imagine a very simple bijective, or one-to-one, transformation that goes from a rectangle to a disk, by taking the Cartesian coordinates, and considering them as polar ones (regardless of potential scalar factors) :

$$x \rightarrow \theta$$

$$y \rightarrow r$$

Applied to one of the most famous portrait in history, here is what happens to the poor Mona:

Fig. 53

Obviously there is more than one way to do that:

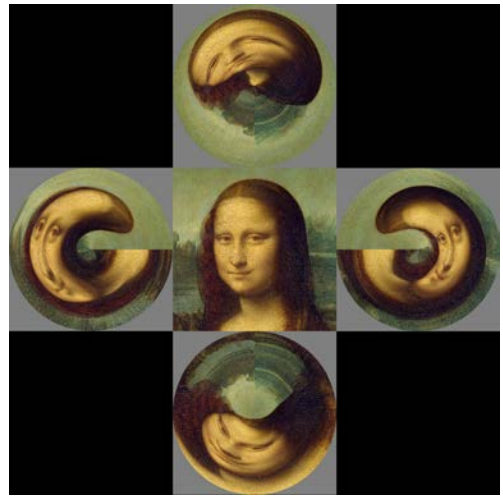

Fig. 54

but we shall stick to this first one.

This transformation turns vertical lines into radials, horizontal lines into concentric circles and oblique lines into one, or many spiral(s):

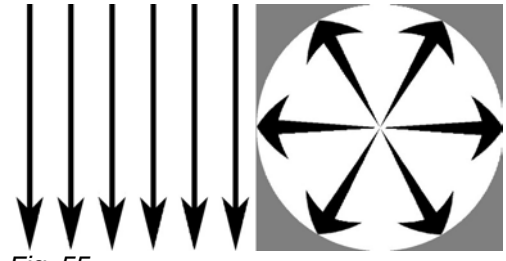

Fig. 55

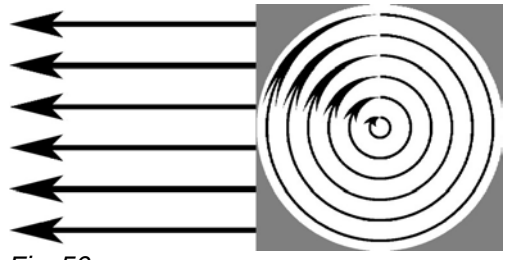

Fig. 56

Fig. 57

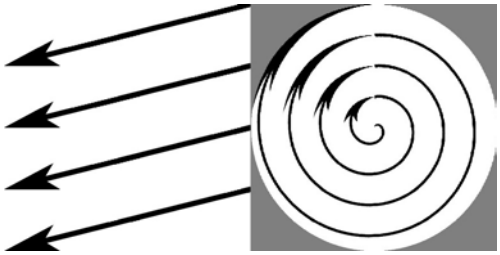

Fig. 58

Fig. 59.

We can now see what happens to classical tessellations:

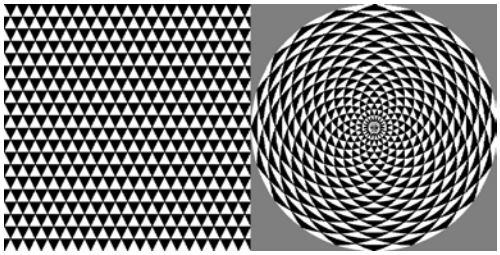

Fig. 60

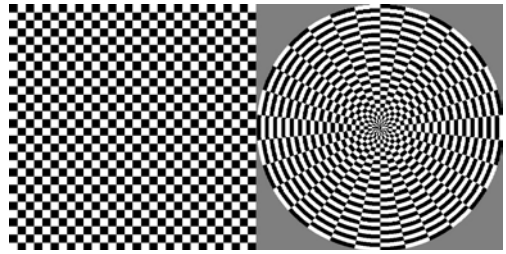

Fig. 61

Contrary to our generalisation of Roman mosaics, the tiles are rounded along concentric circles, which appears more clearly with a smaller number of tiles by layer:

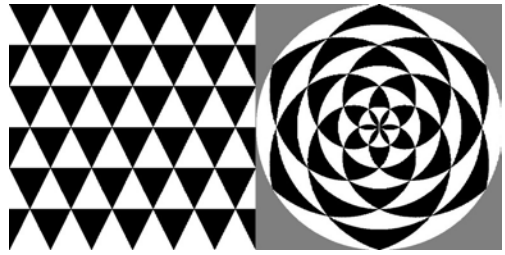

Fig. 62

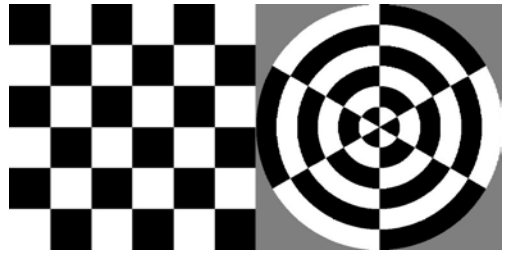

Fig. 63

But, transforming a regular tiling pattern from Cartesian to polar with the simple rule we have adopted, we get tiles that are not isometric, but rather have a constant height, because layers have a constant depth.

It is not the most logical way to tile a disk. It would be more satisfying to get tiles that are isometric. So I wrote another transformation that makes it (regardless

of potential scalar factors) :

$$x \rightarrow \theta$$

$$a^y \rightarrow r$$

Let us see how our new transformation acts upon the same images as before:

Fig. 64

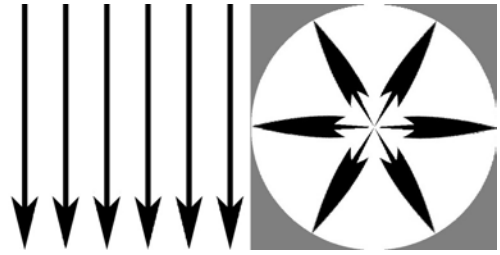

Fig. 65

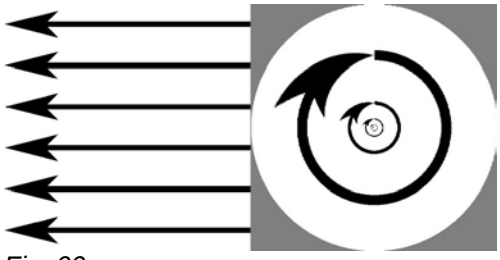

Fig. 66

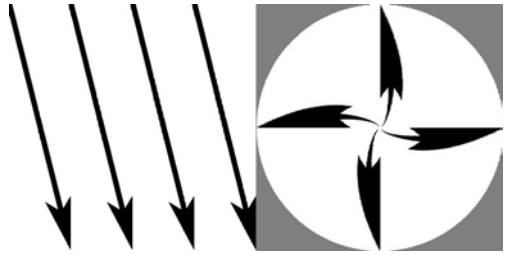

Fig. 67

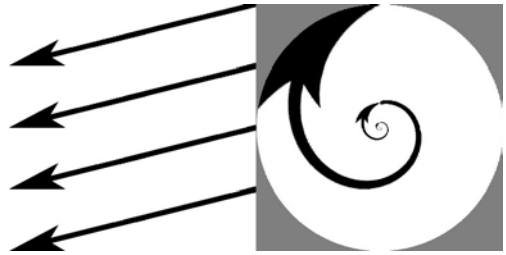

Fig. 68

And now, let us apply this transformation to classical tessellations:

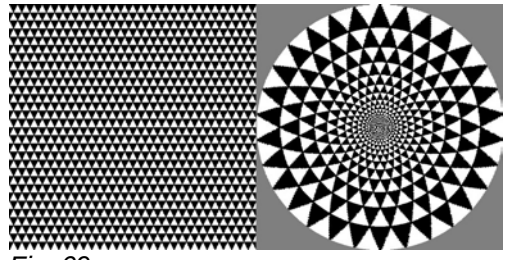

Fig. 69

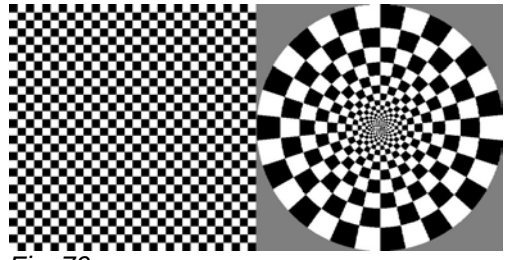

Fig. 70

As with the previous transformation, the tiles have rounded edges:

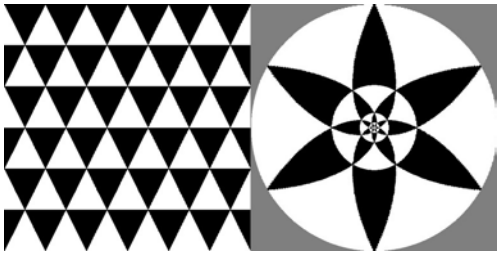

Fig. 71

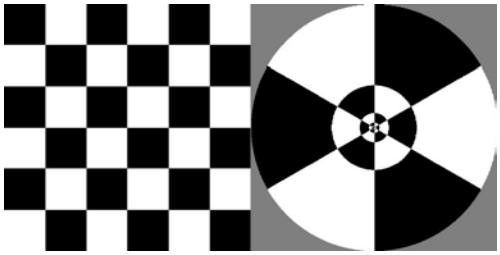

Fig. 72

What one may conclude, among other things, from this little detour, is that spirals are as natural for this geometry of the disk, as oblique straight lines are for our more familiar geometry.

3. Back to phyllotactic spirals

Phyllotactic spirals are phenomena that emerge when florets, or any type of plant organs, appear in a genetic, or generative, spiral. Our non phyllotactic spirals were visible although the basic tiles were arranged, not in a spiral, but in concentric circles.

As a transition, we can make a slight modification to our pattern of 32 triangles for each concentric circle, by converting each circle of tiles into a spiral such as the last tile of each spiral corresponds to the last triangle in the converted circle, but with a radius from the centre increased by the depth of the layer.

Putting triangles in such an arrangement, we could be fooled by the resemblance of the result with our generalisation of the mosaic pattern (see Fig. 33), though by looking more accurately at the centre we discover the truth, the genetic spiral:

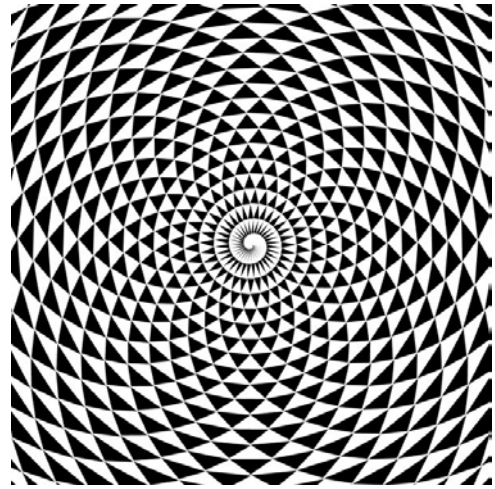

Fig. 73

We see conspicuous spirals as well. There are 32 spirals in the same orientation as the genetic spiral:

Fig. 74

But there are only 31 spirals in the opposite orientation:

Fig. 74

though it is not perceptible with the naked eye…

We are now going to generalise this first experimentation and go closer to true phyllotactic spirals.

All spirals may be written as such:

$r = a\theta^b$

with some particular cases:

$r = a\theta$	*Archimedean*
$r = ab^\theta$	*logarithmic*
$r = a \log b\theta$	*exponential*
$r = a\theta^{1/\varphi}$ ($\varphi = (1+\sqrt{5})/2$)	*golden*
$r = a\theta^{1/2}$ or $a\sqrt{\theta}$	*Fermat or parabolic*

Let us note that, when referring to a mathematical function, the names weirdly are the inverse of those functions…

As we are not interested in drawing whole spirals, but only in putting consecutive particles on a spiral, we take some divergence angle, i. e. the angle between two consecutive particles, as constant (θ_n = n div_angle), and compute the radius r_n given by the adequate formula.

By construction, our first experiment in this part was an Archimedean spiral, with a divergence angle of:

$$(2\pi+{}^{\pi}/_{32}) / 32 = 2\pi\ (65 / 2048)$$

Let us now display this pattern with simple particles:

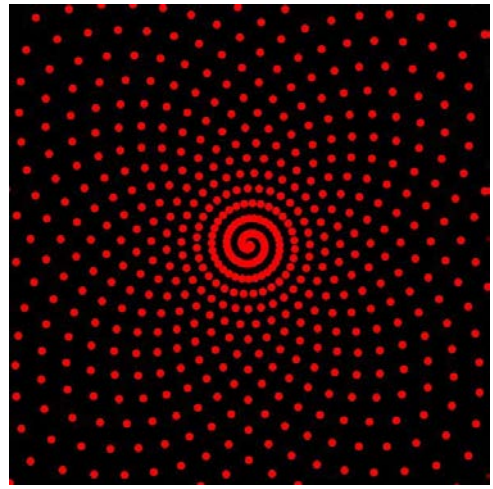

Fig. 75:
Archimedean: $\theta_n = n2\pi\ (65/2048)$ $r_n = 3\theta_n$

The pattern shows obvious spirals, and we could wonder why nature did not chose such a divergence angle… But if we take a smaller value for a (which is the same as pursuing the pattern further), we see that the pattern breaks at some point:

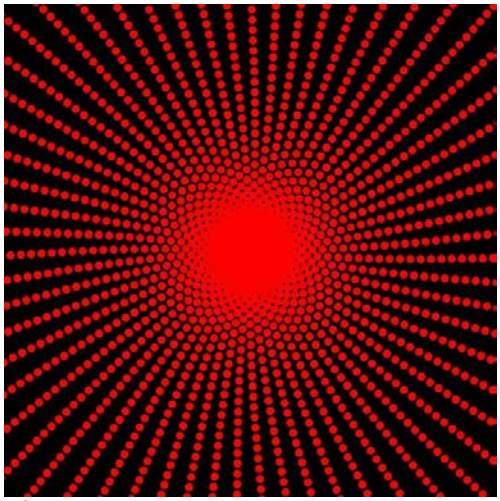

Fig. 76:
Archimedean: $\theta_n=n2\pi\ (65/2048)\ \ r_n=\theta_n$

The spirals “degenerate”.

What is key here, mathematically, is the rationality of the factor of 2π in the divergence angle. Though 65/2048 is irreducible (65 and 2048 are co-prime), this number is undeniably rational.

Yet true phyllotactic spirals emerge when the divergence angle has a factor which is irrational, and among the irrational numbers, the one which is the “most irrational”, if we can say so, is the golden mean, or more precisely here, the factor of the divergence angle is most commonly $1/\varphi^2$ (or $1/(1+\varphi)$) where $\varphi = (1+\sqrt{5})/2$ is the golden mean.

Let us now use this divergence angle for the Archimedean spiral, and we see that the pattern produces phyllotactic spirals:

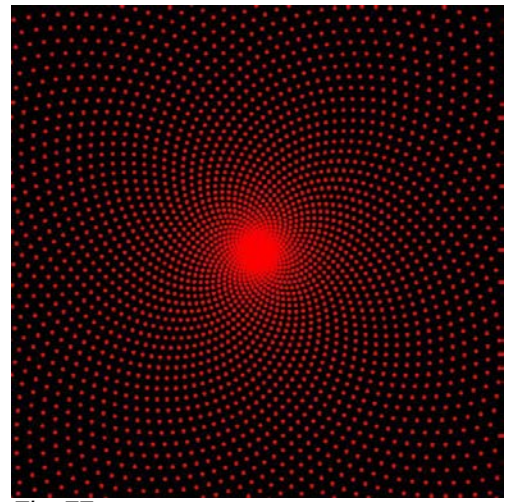

Fig. 77:
Archimedean, $\theta_n=n2\pi/\varphi^2\ \ r_n=0.05\ \theta_n$

Now what about the other types of spirals?

In our non phyllotactic pattern, we used a variation similar to the logarithmic spiral. Let us try it, with the “noble” divergence angle:

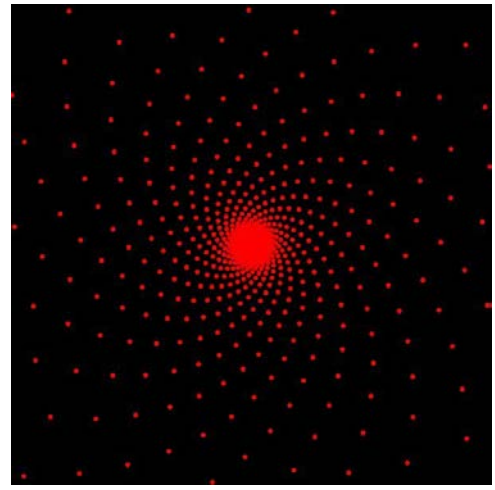

Fig. 78:
Logarithmic: $\theta_n=n2\pi/\varphi^2\ \ r_n=0.005x1.0025^{\theta}$

The pattern is fine but by definition the radius grows exponentially, so it takes a long time to produce the particles in the centre, and they go further from it very rapidly.

Let us now try its reciprocal, the so-called exponential spiral. The phenomenon is inverse from the previous one, particles shoot out very rapidly at the beginning and then more and more slowly:

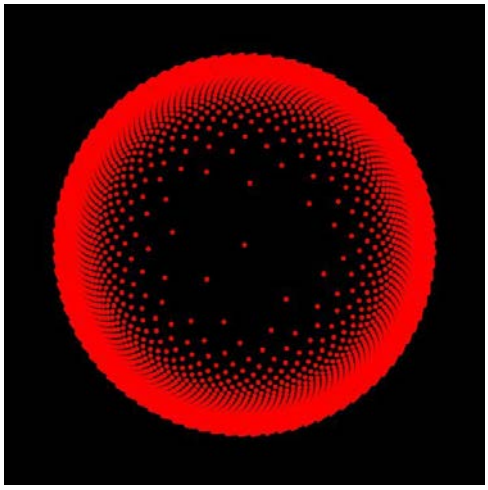

Fig. 79:
Exponential θ_n=n2π/φ² r_n=*20 log(10* θ_n*),*

In those two cases, conspicuous spirals may be hard to discern, though they are actually present.

Let us finish with the two most promising types of spirals, the “golden” one, whose name seems appealing, and then the parabolic or Fermat spiral:

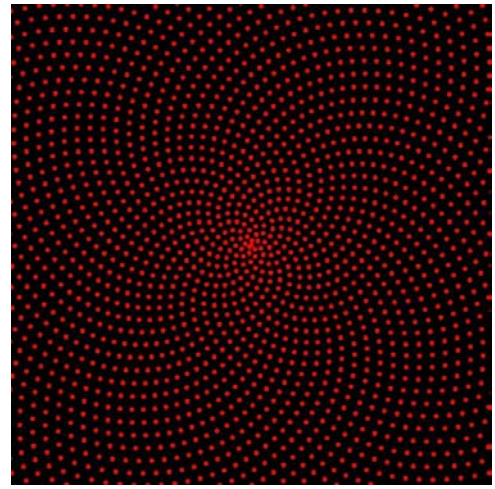

Fig. 80:
Golden: θ_n=n2π/φ² $r_n = 2\ \theta_n^{1/\varphi}$

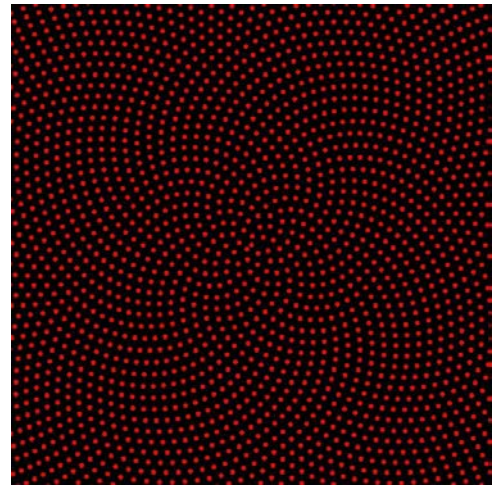

Fig. 81:
Fermat: θ_n=n2π/φ² r_n= 5√θ_n

The two patterns show obvious conspicuous spirals.

Mathematically speaking, all types of genetic spirals yield phyllotactic conspicuous spirals in Fibonacci numbers when the divergence angle is the so-called “noble” one, i. e. 2π/φ². Our interpretation of the Douady-Couder

experiment yielded Archimedean spirals by construction, with the formula:

r = (speed/div_angle) θ.

While the Archimedean, golden and Fermat spirals look a lot like patterns occurring in nature, the logarithmic and exponential ones seem far fetched, and corresponding to very weird behaviours. The golden one has a self-similar propriety, but it does not seem to be a requirement for the kind of behaviour encountered in phyllotactic patterns. Jean [3] does not insist on a particular type of spirals. It depends on a lot of particularities of the plant in question. However, there seems to be a consensus in the scientific community about the Fermat spiral being the type for the daisy and sunflower patterns (see for instance [4]), that goes back to a famous paper by Vogel [5], and like Dimitry Weise insisted upon [6]. The reason invoked in general is the packing efficiency of this pattern. But this efficiency supposes at least two prerequisites: first that the florets, or any shapes in question lie on a plane, secondly that the florets are all of the same size, or that we know of their rate, or rule, of growing, and those prerequisites are not so obvious.

In conclusion, spirals are inherent to the geometry of the disk. Though each type of spiral has its own characteristics, phyllotactic spirals emerge as soon as there is a genetic spiral of any type, and, most importantly, a particular so-called “noble” divergence angle.

Let us finish with enhancing the conspicuous spirals with the Fermat type:

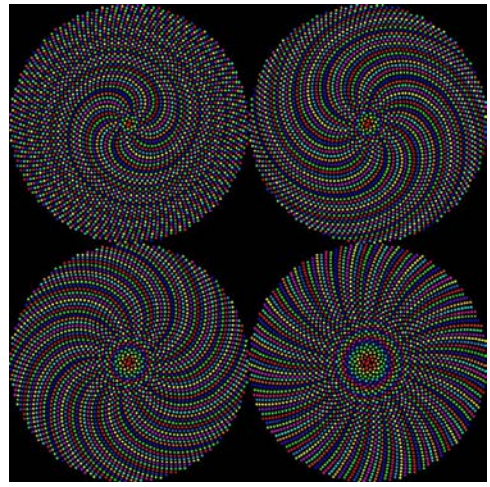

Fig. 82: 34, 55, 89 and 144 conspicuous Fermat spirals.

References

[1] Marie-Pascale Corcuff, “Distant Forces generating Forces”, *GA2018.*

[2] S. Douady, Y. Couder, “Phyllotaxis as a Physical Self-Organized Growth Process”, Physical Review Letters, Volume 68, Number 13, 30 March 1992.

[3] Roger V. Jean, *Phyllotaxis. A Systemic Study in Plant Morphogenesis*, Cambridge University Press, 1994.

[4] Akio Hizume, Takamichi Sushida, Yoshikazu Yamagishi, “Voronoi Phyllotaxis Tiling on the Fermat Spiral”, *Bridges 2014*

[5 Helmut Vogel, “A better way to construct the sunflower head”, *Mathematical Biosciences* 44 (1979), no.3-4, 179–182.

[6] Dimitry L. Weise, “Phyllotaxis is not logarithmic”, *GA2021.*